Laser Enhanced Direct Print Additive Manufacturing for Mm-Wave Components and Packaging

Eduardo A. Rojas-Nastrucci[1], Ramiro Ramirez[1], Derar Hawatmeh[1], Di Lan[1], Jing Wang[1] and Thomas Weller[1]

Abstract **– Direct print additive manufacturing (DPAM) is an additive manufacturing technique that combines fused deposition modeling with micro-dispensing. As a multi-material 3D printing method it has proven to be effective for fabricating printed electronics that operate in the microwave frequency range. This paper discusses the addition of picosecond laser processing to the DPAM process, and the enhancements to high-frequency performance and design capability that are made possible. The use of laser-enhanced DPAM for 3D fabrication of transmission lines, passive components and packaging is discussed.**

1 INTRODUCTION

The use of additive manufacturing (AM) for microwave and mm-wave applications is increasing as improvements in material properties and process control are made. A wide variety of options are available that involve jetting, spraying or dispensing materials into digitally-controlled patterns, followed by some post-processing for curing, surface treatment and/or metallization, e.g. through plating. These options include techniques such as binder-jetting, Polyjet, and aerosol jet. Other AM techniques with proven merits for high-frequency components include laser-based approaches such as selective laser melting and selective laser sintering [1], and Stereolithography [2]. Structures fabricated with these methods are typically all metal, all dielectric, or dielectric with a blanket metal deposition that is not patterned. In some cases, metal traces are 3D printed on substrates that are not produced with AM.

For those applications where it is desirable to use a fully-AM process for printed electronics that require both insulating and conducting layers, printing techniques that seamlessly integrate multi-material deposition capabilities are advantageous. One important advantage is the potential ability to deposit diverse materials without removing the structure from the printing tool; this simplifies layer-to-layer registration, and improves process control when optimizing to eliminate adhesion, delamination, or other problems. The multi-material deposition capability also provides greater freedom in building true 3D structures, rather than stacks of 2D structures which are more practical if multiple tools are in use. Both advantages naturally rely on being able to dry or cure the materials in situ, e.g. with heat, a laser or a UV source.

The inkjet technique is one multi-material AM approach that has been used to fabricate circuits such as substrate-supported antennas and microwave packaging [3]. Another multi-material method is direct print additive manufacturing (DPAM), which combines fused deposition modeling (FDM) of thermoplastics with micro-dispensing of pastes on a common platform. Whereas thin, 0.5 – 5 micron-thick layers are characteristic of the inkjet technique, the typical layer thickness with DPAM is 25-50 microns. This difference makes DPAM more useful for building up larger 3D structures, while inkjet holds the advantage in minimum feature size. Minimum feature size with inkjet and DPAM is approximately 1 and 25 microns, respectively.

In this work, the use of pulsed picosecond laser post-processing is examined as a means to enhance the capabilities of DPAM. One immediate advantage is the ability to achieve smaller feature sizes, and thus extend the upper-frequency range for DPAM components. It has also been observed that laser processing can produce a controlled region of melting within silver-flake conductive pastes, which leads to increased conductivity and thus lower transmission line loss. The ability to precisely control material removal can also be leveraged for the integration of vertical interconnects and packaging of monolithic integrated circuits into 3D printed structures, with low parasitic effects. Finally, the new laser-enhanced DPAM process enables high-frequency transmission lines to be flexibly integrated onto 3D structures. Examples in each of these areas are described in the following sections of the paper.

2 LASER-ENHANCED DIRECT PRINT ADDITIVE MANUFACTURING PROCESS

The fabrication of the components described in this work is done using a single machine, an nScrypt 3Dn tabletop system. This equipment is capable of 3D-printing a wide range of thermoplastics by FDM [4], micro-dispensing conductive pastes, and performing laser processing. The conductive paste used in this work is Dupont CB028, which has a DC conductivity of around 4 MS/m. The picosecond laser machining described in the following sections is performed with a beam that is focused to a 16 μm spot diameter. The laser wavelength is 1064 nm, and the duration of the pulse is <15 ps.

Acrylonitrile butadiene styrene (ABS) is used as a dielectric material, which has a dielectric constant of 2.35 and a loss tangent 0.0065 at 30 GHz [5]. This

[1] Department of Electrical Engineering, University of South Florida, 4202 E. Fowler Avenue, ENB 1118, Tampa, Florida, USA 33620
e-mail: eduardor@mail.usf.edu, ramiror@mail.usf.edu, derar@mail.usf.edu, dilan@mail.usf.edu, jingw@usf.edu, weller@usf.edu

thermoplastic is printed with a nozzle with an inner diameter of 200 µm, which is heated at 230°C, and a printing bed set at 110°C. The ABS layer thickness is 100 µm. The conductive layers of CB028 are micro-dispensed using a 125 µm inner diameter tip, with a speed of 25 mm/s, pressure of 14 psi, and a printing height of 100 µm over the substrate. The printed CB028 is simultaneously dried, since the hot bed heats the part.

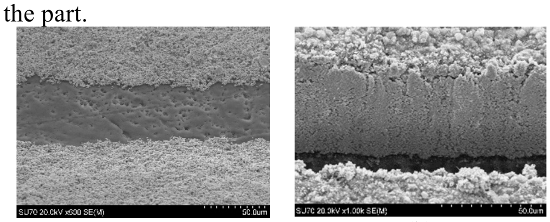

(a) (b)

Figure 1. Tilted top view of slot on CB028 layer. (a) Micro-dispensed slot. (b) Laser machined slot [6].

3 ADVANCEMENTS IN CIRCUIT PERFORMANCE

3.1 Mm-Wave Transmission Lines

One of the main challenges that AM for RF components faces is the relatively high losses of the interconnects, mostly due to the low conductivity and inhomogeneity of the micro-dispensed silver pastes [7]. It has been shown that picosecond laser processing of CB028 layers generates localized solidification of the silver flakes, leading to a great improvement is loss [6]. Fig. 1 shows a comparison of SEM images of a micro-dispensed 50 µm wide slot (Fig. 1.a), and one of the same size realized with picosecond laser machining (Fig. 1.b). It is observed, from cross-section SEM images of the laser machined slots, that the laser beam solidified an area of 2 µm on the CB028 slot walls. This localized solidification of silver produced an improvement in the loss of a coplanar waveguide (CPW) interconnect [6] that is shown in Fig. 2(a). The laser machining technique enables the fabrication of mm-wave interconnects, as shown in Fig. 2(b), since slot widths down to 16 µm are achievable.

3.2 Thru Vias and Packaging

As noted above, DPAM is a low temperature process that enables the fabrication and packaging with lateral interconnection of MMIC (monolithic microwave integrated circuit) dies [8]. Fig. 3 shows a distributed low noise amplifier (LNA) cascaded with a transistor-based tunable band pass filter. Both dies are embedded within a 100 µm deep laser machined cavity over a 3D-printed ABS substrate and interconnected using micro-dispensed, laser-defined microstrip transmission lines.

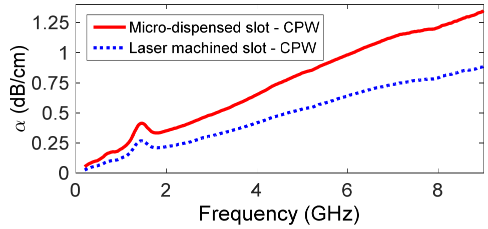

(a)

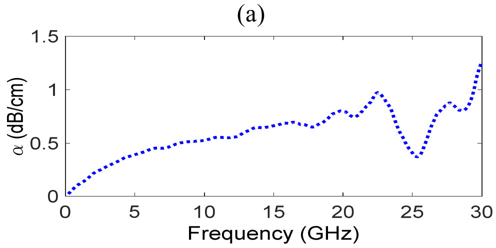

(b)

Figure 2. Measured loss of CPW: (a) micro-dispensed and laser machined 50 µm wide slots. (b) Laser machined 20 µm wide slots [6].

Fig 4. shows the measured S-parameters of the stand-alone GaAs pHEMT LNA (solid), stand-alone GaAs Filter (dashed) and the cascaded response (dotted). This measurement is performed by RF probing directly into the package. The LNA exhibits a gain of 11dB +- 0.5 dB ripple from 2 to 10 GHz along with 1.8 VSWR for both input and output terminals. The transistor based bandpass filter shows a resonant frequency centered at 5 GHz with a return loss greater than 30 dB and 0.52 dB insertion loss as shown in Fig. 4(a) and Fig. 4(b), respectively. The measured insertion loss due to the 3D printed overall package interconnections is 0.2 dB at 7 GHz.

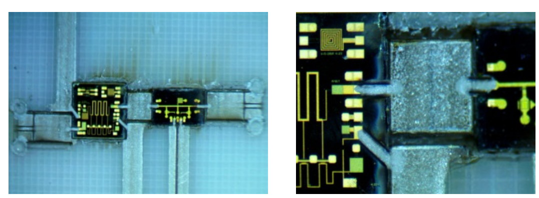

Figure 3: Cascaded MMIC LNA and filter (left), RF Lateral interconnection close-up (right).

Vertical interconnects are fabricated using the DPAM technology, by taking advantage of the precise laser machining of the ABS substrate. For this, an ABS substrate is printed, then a 50 µm thick layer of CB028 is micro-dispensed, and another layer of ABS (200 µm thick in this case) is deposited. This stack is then laser machined with a power setting of 0.8 W, which leads to an etch rate of around 10 µm per pass. Fig. 5(a) shows a diagram of the via with dimensions 200 µm x 200 µm x 200 µm (width, length, and depth). Fig. 5(b) shows the machined cavity, and the CB028 bottom layer which can be appreciated with a darker color, and where laser marks can be identified. The top surface of the ABS substrate appears as a bright white color. This cavity is filed with CB028 using micro-dispensing (Fig. 5.b), obtaining a thru via with a measured DC resistance of less than 0.1 Ω.

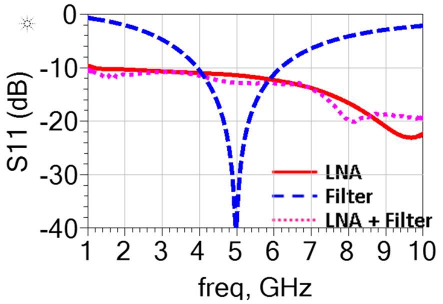

(a)

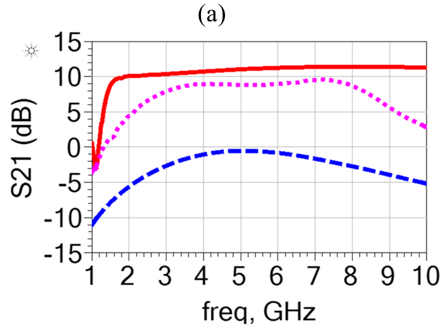

(b)

Figure 4: (a) Measured input reflection coefficient and (b) transmission coefficient.

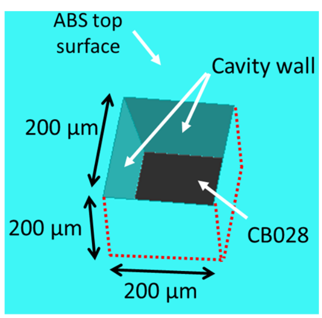

(a)

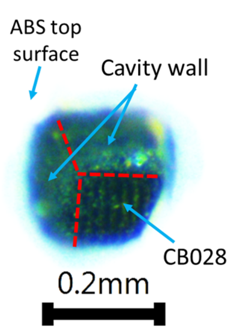

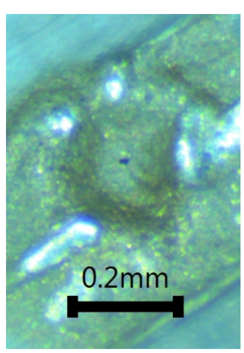

(b) (c)

Figure 5: (a) Diagram of the thru via.
(b) Micrograph of the laser machined cavity (tilted top view. (b) Thru via filed with CB028.

3.3 3D Component Integration

The previously described processes enable the direct interconnection of 3D structures and transmission lines, which can then also be integrated with MMIC dies and connectors. One example of this integration is the capacitively-loaded evanescent-mode cavity resonator shown in Fig. 6. This resonator is conformed by a cavity that is 3D printed using FDM, and is then coated with CB028. This cavity has a post inside, which is in contact with the bottom layer of conductor, and is capacitively coupled with the top layer of conductor. The resonance frequency can be tuned by changing the post coupling capacitance, by, for example, changing the gap size.

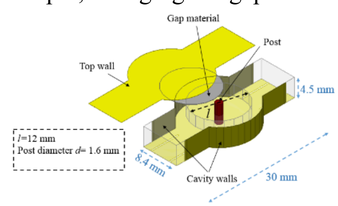

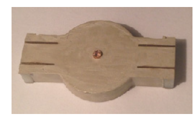

(a) (b)

Figure 6: (a) Geometry of the cavity resonator.
(b) Fabricated component [9].

The described resonator structure is excited by CPW-like transmission lines, as shown in Fig. 6(b). These feed lines are patterned in the CB028 layer using the pulsed laser machining process. Most of the current in this structure is concentrated on the CPW end close to the post (Fig. 7(a)), therefore, taking advantage of the laser processing effects of increased conductivity. The other area where the current concentrates is the post itself (Fig. 7(b)). The measured Q-factor ranges from 107 to 140, in a resonance frequency range of 2.3 GHz -7 GHz [9].

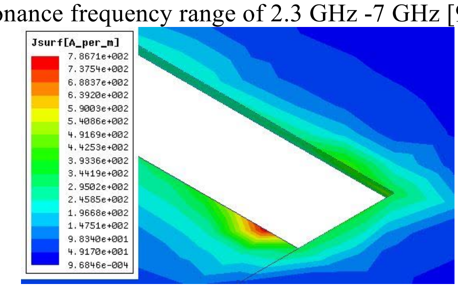

(a)

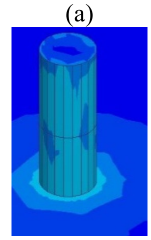

(b)

Figure 7: Simulated current densities on the resonator. (a) On the interconnect next to the post.
(b) On the post.

3 Conclusion

It is shown that by employing DPAM it is possible to fabricate multilayer packaging, integration of MMIC dies, and interconnection of 3D structures, using a single tool. Improvements made in feature size and the conductivity of the metal-loaded pastes thru pulsed laser processing have enabled performance improvements and an increase of operating frequency into the mm-wave range.

Acknowledgments

This work was supported in part by the National Science Foundation under Grant No. ECCS-1232183.

References

[1] O. A. Peverini, M. Lumia, F. Calignano, G. Addamo, M. Lorusso, E. P. Ambrosio*, et al.*, "Selective Laser Melting Manufacturing of Microwave Waveguide Devices," *Proc. IEEE,* vol. 105, pp. 620-631, Apr. 2017.

[2] C. Guo, X. Shang, J. Li, F. Zhang, M. J. Lancaster, and J. Xu, "A Lightweight 3-D Printed X-Band Bandpass Filter Based on Spherical Dual-Mode Resonators," *IEEE Microw. Compon. Lett.,* vol. 26, pp. 568-570, 2016.

[3] W. Su, B. S. Cook, and M. M. Tentzeris, "Additively Manufactured Microfluidics-Based "Peel-and-Replace" RF Sensors for Wearable Applications," *IEEE Transactions on Microwave Theory and Techniques,* vol. 64, pp. 1928-1936, 2016.

[4] J. Castro, E. A. Rojas-Nastrucci, A. Ross, T. M. Weller, and J. Wang, "Fabrication, Modeling, and Application of Ceramic-Thermoplastic Composites for Fused Deposition Modeling of Microwave Components," *IEEE Transactions on Microwave Theory and Techniques,* vol. 65, pp. 2073-2084, 2017.

[5] A. Vera López, E. A. Rojas-Nastrucci, M. Córdoba-Erazo, T. Weller, and J. Papapolymerou, "Ka-Band Characterization and RF Design of Acrylonitrile Butadiene Styrene (ABS)," presented at the 2015 IEEE MTT-S International Microwave Symposium (IMS), 2015.

[6] E. A. Rojas-Nastrucci, H. Tsang, P. I. Deffenbaugh, R. A. Ramirez, D. Hawatmeh, A. Ross*, et al.*, "Characterization and Modeling of K-Band Coplanar Waveguides Digitally Manufactured Using Pulsed Picosecond Laser Machining of Thick-Film Conductive Paste," *IEEE Transactions on Microwave Theory and Techniques,* vol. PP, pp. 1-8, 2017.

[7] T. P. Ketterl, "A 2.45 GHz Phased Array Antenna Unit Cell Fabricated Using 3-D Multi-Layer Direct Digital Manufacturing," *IEEE Trans. Microw. Theory Techn.,* vol. 63, No. 12, pp. 4382-4394, Dec. 2015.

[8] R. A. Ramirez, D. Lan, J. Wang, and T. M. Weller, "MMIC Packaging and On-Chip Low-Loss Lateral Interconnection using Additive Manufacturing and Laser Machining," in *2017 IEEE MTT-S International Microwave Symposium (IMS)*, 2017.

[9] D. Hawatmeh and T. Weller, "A S/C-Band High Q Resonator Architecture for Direct Print Additive Manufacturing," in *IEEE WAMICON 2017*, Cocoa Beach, FL, 2017.